*Inorg. Chem.* **2003**, *42*, 5551–5559

# Electrochemical and Spectroscopic Characterization of the Novel Charge-Transfer Ground State in Diimine Complexes of Ytterbocene

**Ryan E. Da Re,[†] Christopher J. Kuehl,[†] Mac G. Brown,[‡] Reginaldo C. Rocha,[‡] Eric D. Bauer,[§] Kevin D. John,[†] David E. Morris,*[,†] Andrew P. Shreve,[‡] and John L. Sarrao[§]**

*Chemistry Division, Bioscience Division, and Materials Science and Technology Division, Los Alamos National Laboratory, Los Alamos, New Mexico 87545*

Received February 19, 2003

The novel charge-transfer ground state found in α,α′-diimine adducts of ytterbocene $(C_5Me_5)_2Yb(L)$ [L = 2,2′-bipyridine (bpy) and 1,10-phenanthroline (phen)] in which an electron is spontaneously transferred from the $f^{14}$ metal center into the lowest unoccupied ($\pi^*$) molecular orbital (LUMO) of the diimine ligand to give an $f^{13}$–$L^{\bullet-}$ ground-state electronic configuration has been characterized by cyclic voltammetry, UV–vis–near-IR electronic absorption, and resonance Raman spectroscopies. The voltammetric data demonstrate that the diimine ligand LUMO is stabilized and the metal f orbital is destabilized by ∼1.0 V each upon complexation for both bpy and phen adducts. The separation between the ligand-based oxidation wave ($L^{0/-}$) and the metal-based reduction wave ($Yb^{3+/2+}$) in the ytterbocene adducts is 0.79 V for both bpy and phen complexes. The UV–vis–near-IR absorption spectroscopic data for both the neutral adducts and the one-electron-oxidized complexes are consistent with those reported recently, but previously unreported bands in the near-IR have been recorded and assigned to ligand ($\pi^*$)-to-metal (f orbital) charge-transfer (LMCT) transitions. These optical electronic excited states are the converse of the ground-state charge-transfer process (e.g., $f^{13}$–$L^{\bullet-} \leftrightarrow f^{14}$–$L^0$). These new bands occur at ∼5000 $cm^{-1}$ in both adducts, consistent with predictions from electrochemical data, and the spacings of the resolved vibronic bands in these transitions are consistent with the removal of an electron from the ligand $\pi^*$ orbital. The unusually large intensity observed in the f → f intraconfiguration transitions for the neutral phenanthroline adduct is discussed in terms of an intensity-borrowing mechanism involving the low-energy LMCT states. Raman vibrational data clearly reveal resonance enhancement for excitation into the low-lying $\pi^* \rightarrow \pi^*$ ligand-localized excited states, and comparison of the vibrational energies with those reported for alkali-metal-reduced diimine ligands confirms that the ligands in the adducts are reduced radical anions. Differences in the resonance enhancement pattern for the modes in the bipyridine adduct with excitation into different $\pi^* \rightarrow \pi^*$ levels illustrate the different nodal structures that exist in the various low-lying $\pi^*$ orbitals.

## Introduction

The adducts of $(C_5Me_5)_2Yb$ (ytterbocene) with α,α′-diimine ligands including 2,2′-bipyridine (bpy) and 1,10-phenanthroline (phen) have recently been reported to have a novel ground-state electronic configuration in which the formally $f^{14}$ Yb(II) metal center transfers an electron into the lowest unoccupied molecular orbital (LUMO) of the coordinated diimine ligand to give intensely colored species whose bulk properties (magnetic susceptibility, $^1$H NMR, IR, UV−vis, and X-ray crystallography) are consistent with a paramagnetic complex containing an oxidized ($f^{13}$) metal center and a radical anion on the diimine ligand.[1] Similar behavior was previously postulated for the samarocene adduct with bipyridine $[(C_5Me_5)_2Sm(bpy)]$.[2] However, the behavior for these diimine adducts is in contrast to that seen for the structurally homologous bis(pyridine) adduct of ytterbocene $[(C_5Me_5)_2Yb(py)_2]$, which has a diamagnetic ($f^{14}$

* Author to whom correspondence should be addressed. E-mail: demorris@lanl.gov.
† Chemistry Division.
‡ Bioscience Division.
§ Materials Science and Technology Division.

(1) Schultz, M.; Boncella, J. M.; Berg, D. J.; Tilley, T. D.; Andersen, R. A. *Organometallics* **2002**, *21*, 460−472.
(2) Evans, W. J.; Drummond, D. K. *J. Am. Chem. Soc.* **1989**, *111*, 3329−3335.

10.1021/ic030069i CCC: $25.00 
Published on Web 08/05/2003

metal−neutral ligand) ground state. The novel charge-transfer ground-state behavior has now been elaborated synthetically for a number of additional N-heterocyclic ligands including several bridging ligands that can afford dimeric ytterbocene structures.[3] This prior work illustrates the generality of the ground-state metal-to-ligand charge-transfer phenomenon, but leaves open a fundamentally interesting question as to its origin.

The magnetic properties of these systems have been investigated extensively by variable-temperature and variable-field-strength magnetic susceptibility.[1,3] These experiments clearly illustrate that the spin systems on the oxidized metal(s) and the reduced ligand are correlated and indicate some interesting variations in the extent of coupling between the spin systems that suggest a molecular and/or electronic structural basis for the variability. For example, the room-temperature magnetic moments ($\mu$) determined for the bpy and phen complexes are both lower than would be predicted for noninteracting metal-centered $^2F_{7/2}$ ($f^{13}$) and ligand-centered $^2S_{1/2}$ ($(\pi^*)^1$) spin states, and $\mu$ for the bpy complex is significantly lower than that for the phen complex. Treatment of these data using the empirical model of Kahn[4,5] led to the conclusion that the spin systems on the metal and ligand are antiferromagnetically coupled for both the bpy and phen complexes, but this approach does not permit the determination of the magnitude of the coupling. In general, no systematic trends related to the diimine ligand structures or redox energetics have been identified yet that shed light on the origin of the charge-transfer process per se or the resulting spin interactions.

The present work was undertaken in an effort to further describe the structural and energetic properties that exist in the charge-transfer ground state of these complexes and to attempt to gain additional insight into the origin of the effect. Here we report detailed cyclic voltammetric, UV−vis−near-IR electronic absorption, and resonance Raman spectroscopic data for the neutral parent (charge-transfer) complex and the one-electron-oxidized species of the bipyridine and phenanthroline adducts of ytterbocene.

## Experimental Section

**Syntheses.** All reactions and product manipulations were carried out under a dry helium atmosphere using standard drybox techniques. Toluene, tetrahydrofuran (THF), and diethyl ether were dried and deoxygenated by distillation from sodium benzophenone ketyl under nitrogen prior to use. Dichloromethane was distilled from $CaH_2$ under a dry nitrogen atmosphere. 2,2′-Bipyridine and 1,10-phenanthroline were purchased commercially and purified by sublimation. $(C_5Me_5)_2Yb(OEt_2)$, $(C_5Me_5)_2Yb(py)_2$, $(C_5Me_5)_2Yb$(bpy), and $(C_5Me_5)_2Yb$(phen) were prepared according to published procedures.[1] The cationic adducts $[(C_5Me_5)_2Yb(bpy)]^+$ and $[(C_5Me_5)_2Yb(phen)]^+$ were prepared as the $PF_6^-$ salts by oxidation of their respective neutral adducts with $[(C_5H_5)_2Fe]PF_6$ (Aldrich).

**Electrochemistry.** Cyclic voltammetric studies were conducted in a Vacuum Atmosphere inert atmosphere glovebox (nitrogen or helium) using a Perkin-Elmer Princeton Applied Research Corp. (PARC) model 263 potentiostat under computer control using M270 software. The electrochemical cell was a modified PARC microcell consisting of a ∼3 mm platinum disk working electrode, a Pt wire counter electrode, and a silver wire quasi-reference electrode. All experiments were conducted in purified THF using ∼0.1 M $[(n\text{-}C_4H_9)_4N][B(C_6F_5)_4]$ as the supporting electrolyte. The benefits of this electrolyte for reducing uncompensated resistance in low-dielectric-constant solvents such as THF have been previously described.[6,7] Measured potentials were calibrated using the ferrocenium/ferrocene couple ($E_{1/2} \approx 0.55$ V vs NHE). Data were analyzed using the IGOR Pro (Wavemetrics, Inc.) software package on a Macintosh platform.

**Electronic Absorption Spectroscopy.** Electronic absorption spectra from 300 to 2200 nm were recorded at room temperature using a Perkin-Elmer Lambda 19 spectrophotometer. Spectra of $Yb(C_5Me_5)_2$(bipy) and $Yb(C_5Me_5)_2$(phen) were obtained in both toluene-$h_8$ and toluene-$d_8$ to enable spectral subtraction of absorbances from solvent vibrational overtone bands and thereby derive continuous traces attributable solely to the ytterbocene complexes. A pair of 1 mm path length quartz spectrophotometric cells were used in the region $\lambda > 2000$ nm to minimize contributions from these overtone bands.

**Raman Spectroscopy.** Raman spectra were obtained in a backscattering geometry from samples sealed in capillaries. Either 514 nm excitation from an Ar ion laser source (Coherent Innova 400) or 753 nm excitation from an Ar ion-pumped Ti:sapphire laser (Spectra Physics model 3900) was used. In the former case, scattered light was collected, passed through a holographic notch filter (Kaiser), and directed into a 1 m spectrograph (SPEX 1702) and onto a liquid-nitrogen-cooled charge-coupled device (CCD) detector (Princeton Instruments). In the latter case, light was collected and passed through a triple spectrometer (SPEX 1877) onto a liquid-nitrogen-cooled CCD (Princeton Instruments). Typical excitation powers were 12−15 mW, and typical integration times to obtain spectra were 5−10 min. Spectra were calibrated using known spectral lines from low-intensity calibration lamps.

## Results and Discussion

**Electrochemistry.** Redox potentials in multivalent redox-active systems such as these ytterbocene adducts provide an important means to assess the stabilization of charge-transfer ground states with respect to the nominal oxidation states of the constituents (e.g., the $Yb^{3+/2+}$ couple in the ytterbocene moiety and the $L^{0/-}$ couple in the diimine ligand). Shifts in the redox potentials of both metal-based and ligand-based couples upon coordination are common and provide a direct measure of the perturbations in orbital energies as a result of the complex formation. In addition, differences in electrochemical potentials between metal-localized and ligand-localized redox processes are generally correlated with the energies of the corresponding optically promoted charge-transfer transitions.[8,9] Thus, in these ytterbocene adducts the ligand ($\pi^*$)-to-metal (f orbital) optical charge-transfer transi-

(3) Berg, D. J.; Boncella, J. M.; Andersen, R. A. *Organometallics* **2002**, *21*, 4622−4631.
(4) Kahn, M. L.; Sutter, J.-P.; Golhen, S.; Guionneau, P.; Ouahab, L.; Kahn, O.; Chasseau, D. *J. Am. Chem. Soc.* **2000**, *122*, 3413−3421.
(5) Kahn, M. L.; Sutter, J.-P.; Golhen, S.; Guionneau, P.; Ouahab, L.; Kahn, O.; Chasseau, D. *J. Am. Chem. Soc.* **2000**, *122*, 9566−9566.
(6) LeSuer, R. J.; Geiger, W. E. *Angew. Chem., Int. Ed.* **2000**, *39*, 248−250.
(7) Camire, N.; Mueller-Westerhoff, U. T.; Geiger, W. E. *J. Organomet. Chem.* **2001**, *637*, 823−826.
(8) Ohsawa, Y.; Hanck, K. W.; DeArmond, M. K. *J. Electroanal. Chem.* **1984**, *175*, 229−240.

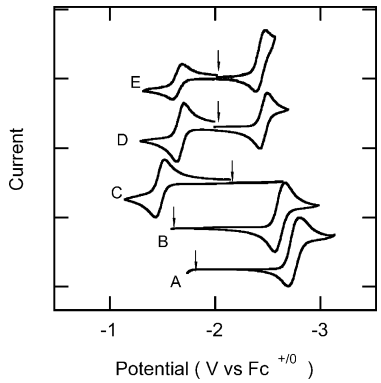


**Figure 1.** Cyclic voltammograms at a Pt disk working electrode in ~0.1 M [(*n*-$C_4H_9)_4N$][$B(C_6F_5)_4$]/THF at room temperature: (A) 2,2′-bipyridine; (B) 1,10-phenanthroline; (C) $(C_5Me_5)_2Yb(THF)_n$; (D) $(C_5Me_5)_2Yb$(bpy); (E) $(C_5Me_5)_2Yb$(phen). Concentrations of all analytes were ~5 mM except for $(C_5Me_5)_2Yb$(phen), which was solubility limited to ~1 mM. Currents are in arbitrary units to facilitate comparisons. The rest potential for each system (potential at which there is zero net current flow) is indicated by the vertical arrow.

**Table 1.** Measured Redox Potentials for $(C_5Me_5)_2Yb$ Adducts and Constituents[a]

| species | $E_{1/2}(L^{0/-})$ | $\Delta E_1$[b] | $E_{1/2}(M^{3+/2+})$ | $\Delta E_2$[c] | $\Delta E_c$[d] | log $K_c$[e] |
|---|---|---|---|---|---|---|
| $(C_5Me_5)_2Yb(THF)_n$ | | | −1.48 | | | |
| bpy | −2.75 | | | | | |
| $(C_5Me_5)_2Yb$(bpy) | −1.67 | 1.08 | −2.46 | −0.98 | 0.79 | 13.4 |
| phen | −2.61 | | | | | |
| $(C_5Me_5)_2Yb$(phen) | −1.64 | 0.97 | −2.43 | −0.95 | 0.79 | 13.4 |

[a] All measured $E_{1/2}$ values are in volts versus $[(C_5H_5)_2Fe]^{+/0}$ in 0.1 M TBA[$B(C_6F_5)_4$]/THF. [b] $\Delta E_1 = E_{1/2}$(complexed ligand) − $E_{1/2}$(free ligand). [c] $\Delta E_2 = E_{1/2}(M^{3+/2+}$ in THF adduct) − $E_{1/2}(M^{3+/2+}$ in diimine adduct). [d] $\Delta E_c = E_{1/2}(L^{0/-}) - E_{1/2}(M^{3+/2+})$. [e] $K_c = 10^{(\Delta E_c/59\ mV)}$ for the reaction given in eq 1 ref 10.

tion, which is the converse of the spontaneous process responsible for creating the charge-transfer ground state, should correlate with the difference in redox potentials, eq 1. Finally, the redox potentials also provide a measure of

$$\Delta[|E_{1/2}(\text{diimine}^{0/-}) - E_{1/2}(Yb^{3+/2+})|] \approx \Delta E\{[(\pi^*)^1(f)^{13}] \rightarrow [(\pi^*)^0(f)^{14}]\} \quad (1)$$

the stabilization of the charge-transfer state with respect to the comproportionation equilibrium between the fully oxidized and fully reduced states of the system.[10] This is well documented in systems such as the Creutz−Taube ion ($[(NH_3)_5Ru^{II}$(pyrazine)$Ru^{III}(NH_3)_5]^{5+}$), for example, in which the separation between the $Ru^{III-}Ru^{III}/Ru^{III-}Ru^{II}$ couple and the $Ru^{III-}Ru^{II}/Ru^{II-}Ru^{II}$ couple is a direct measure of the stability of the mixed-valent form of the complex.

Typical cyclic voltammetric scans for ~0.1 M [(*n*-$C_4H_9)_4N$][$B(C_6F_5)_4$]/THF solutions of the bpy and phen adducts of $(C_5Me_5)_2Yb$ and for the uncomplexed (neutral) ligands and the ytterbocene precursor $(C_5Me_5)_2Yb(OEt_2)$ are shown in Figure 1. Potential data extracted from these scans are compiled in Table 1. The ytterbocene etherate precursor is an olive green color. When this solid is dissolved in the THF solution, it turns a brilliant cherry red, indicating that the solution species is most likely a THF adduct. An attempt was also made to collect voltammetric data for the diamagnetic bis(pyridine) adduct $(C_5Me_5)_2Yb(py)_2$. This complex is also olive green, but turns deep red on dissolution in THF solution, and the resulting voltammetry is identical to that seen for the etherate precursor in THF, suggesting that THF may also displace coordinated pyridine under the large molar excess of THF to pyridine in these solutions. Addition of excess pyridine to a solution of the etherate complex in THF ultimately produced a pale green solution color (at ~15 equiv of py/equiv of complex), but the voltammetric behavior of this $(C_5Me_5)_2Yb$ plus excess pyridine solution (up to ~100 equiv of py) was essentially the same as that observed for the THF adduct of $(C_5Me_5)_2Yb$.

The voltammetric data for the precursor species (Figure 1, Table 1) clearly demonstrate that the reduced ($f^{14}$) ($C_5Me_5)_2Yb$ precursor has insufficient thermodynamic driving force to reduce either bpy or phen in the absence of a coordination effect as noted previously.[1] However, upon complexation of either diimine ligand, there are significant shifts in the potentials of the voltammetric waves in the system. Note that assignments of the voltammetric waves in the complexes to specific redox transformations cannot be made in the absence of other data. However, given the evidence provided in the previous reports[1,3] and below in support of a spontaneous transfer of an electron from the metal center to the diimine ligand in the ground state of the complex, we can be confident in assigning the voltammetric waves in the complexes to a diimine ligand-based oxidation process and a metal-based reduction process. These assignments establish the remarkable change in the redox energetics in these systems. For both the bpy and phen adducts, the ligand LUMO has been stabilized by ~1 V and the metal has been made more difficult to reduce by ~1 V upon complexation (Table 1). Furthermore, the separation between the two voltammetric waves in the complexes, which is a direct measure of the stability of the charge-transfer ground state, is 0.79 V, which translates into a comproportionation constant for the reaction between the fully oxidized and fully reduced species, eq 2.[10] For comparison, the shift in the

$$(C_5Me_5)_2Yb^{III}(L) + (C_5Me_5)_2Yb^{II}(L^-) \rightleftharpoons 2(C_5Me_5)_2Yb^{III}(L^-) \quad K_c = 10^{13.4} \quad (2)$$

reduction potential upon coordination for bpy and phen in covalent transition-metal complexes such as the trisdiimine chelates of Fe(II) and Ru(II) is ~0.8 V, but the $M^{3+/2+}$ couples are little perturbed upon complexation.[11] There are no published data for ligand-based reduction potentials of diimine ligands coordinated to lanthanides for comparison. It is nonetheless quite remarkable that the stabilization of the ligand LUMOs in these ytterbocene complexes is of the same magnitude as that in covalent transition-metal com-

(9) Morris, D. E.; Ohsawa, Y.; Segers, D. P.; DeArmond, M. K.; Hanck, K. W. *Inorg. Chem.* **1984**, *23*, 3010−3017.
(10) Kaim, W.; Klein, A.; Glöckle, M. *Acc. Chem. Res.* **2000**, *33*, 755−763.
(11) Morris, D. E. *Electrochemical and Electron Spin Resonance Spectroscopic Studies of $d^6$ Transition-Metal Complexes of Imine Ligands*; North Carolina State University: Raleigh, NC, 1984; p 160.

plexes having substantial orbital interactions between the metal and ligand.

Other aspects of the voltammetric behavior for these precursors and the adducts in 0.1 M TBA[$B(C_6F_5)_4$]/THF solution are for the most part unexceptional. All voltammetric waves exhibit behavior with scan rate indicative of simple electron transfer, although the scan rate dependence of the separation between cathodic and anodic peaks in many cases indicates some electron-transfer kinetically limited behavior.[12] For the phen adduct the peak current for the metal-based reduction wave is approximately twice that for the ligand-based oxidation wave at any given scan rate. However, other metrics such as the separation between the peak potentials or between the cathodic peak potential and the potential at half the peak current[12] do not suggest that this wave is a two-electron process. In fact, the scan rate dependence of the separation between cathodic and anodic peaks for the two principal waves in the phen adduct indicates that the kinetics of electron transfer for ligand oxidation are slower than those for metal reduction, and this effect likely accounts for most of the difference in the measured peak currents for the two processes.[12]

For the bpy and phen adducts there is also an additional reduction wave at potentials slightly negative (~300 mV) of the wave assigned to the metal-based reduction. This additional wave has only ~30% of the peak current compared to the principal metal-based and ligand-based waves, but it is reversible. This wave could be due to small amounts of free ligand in the solution since the potential is nearly the same as the reduction potential for the free ligand in pure solution. Alternatively, it could be due to the addition of a second electron to the ligand in the complex. Given the enormous stabilization of the ligand LUMO as indicated by the ligand-based oxidation wave, the addition of a second electron to this LUMO should certainly be possible within the available potential range of the solvent. Similar behavior has been observed in other transition-metal−diimine complexes.[13]

**Electronic Absorption Spectroscopy.** The UV−vis−near-IR electronic absorption spectra of the ytterbocene complexes $[(C_5Me_5)_2Yb(bpy)]^{0/+}$ and $[(C_5Me_5)_2Yb(phen)]^{0/+}$ are shown in Figures 2 (cationic adducts) and 3 (neutral adducts). With the exception of the data collected in the near-infrared region ($\lambda$ > 1100 nm) for the neutral complexes $(C_5Me_5)_2Yb(bpy)$ and $(C_5Me_5)_2Yb(phen)$, which are reported here for the first time, these data are comparable to those reported by Andersen and co-workers.[1]

The electronic absorption spectra of the cations $[(C_5Me_5)_2Yb(bpy)]^+$ and $[(C_5Me_5)_2Yb(phen)]^+$ both exhibit two broad absorption bands in the visible region as well as several sharper features in the region between 9000 and 12500 $cm^{-1}$. The absorptions in the near-infrared region were previously assigned to f → f transitions on the basis of their energies and moderate intensities ($\epsilon \leq 200$);[1] transitions within the

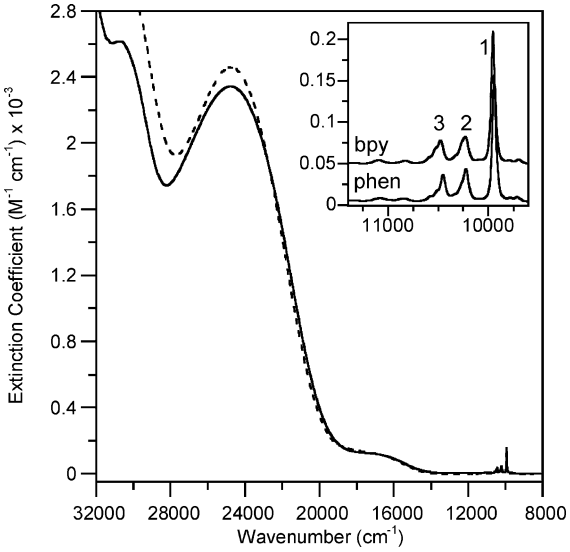


**Figure 2.** UV−vis−near-IR electronic absorption spectra for $[(C_5Me_5)_2Yb(bpy)]^+$ (- - -) and $[(C_5Me_5)_2Yb(phen)]^+$ (—) in $CH_2Cl_2$ solution at 300 K. The spectrum of $(C_5Me_5)_2Yb(bpy)$ shown in the figure inset is vertically offset for clarity.

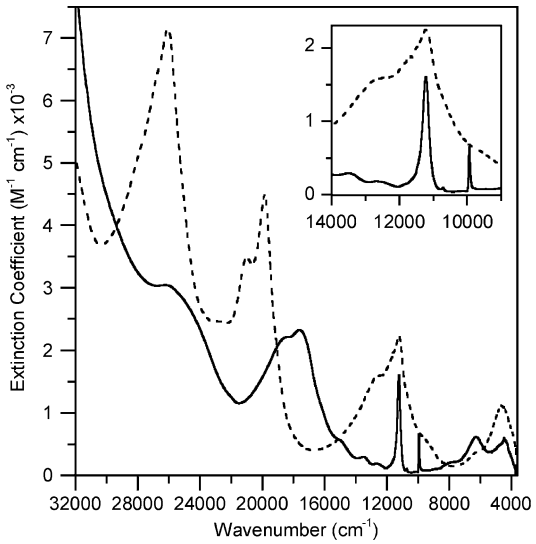


**Figure 3.** UV−vis−near-IR electronic absorption spectra for $(C_5Me_5)_2Yb(bpy)$ (- - -) and $(C_5Me_5)_2Yb(phen)$ (—) in toluene-$h_8$ and -$d_8$ solution at 300 K.

$f^{13}$ electronic configuration of Yb(III) give rise to weak absorption bands that typically occur near 10000 $cm^{-1}$.[14] The remarkable similarities between the electronic spectra of $[(C_5Me_5)_2Yb(bpy)]^+$ and $[(C_5Me_5)_2Yb(phen)]^+$ in this region

(12) Bard, A. J.; Faulkner, L. R. *Electrochemical Methods: Fundamentals and Applications*, 2nd ed.; John Wiley and Sons: New York, 2001.
(13) Ohsawa, Y.; DeArmond, M. K.; Hanck, K. W.; Morris, D. E.; Whitten, D. G.; Neveux, P. E. *J. Am. Chem. Soc.* **1983**, *105*, 6522−6524.

(14) (a) Jiang, H. D.; Wang, J. Y.; Zhang, H. J.; Hu, X. B.; Teng, B.; Zhang, C. Q.; Wang, P. *Chem. Phys. Lett.* **2002**, *357*, 15−19. (b) Jiang, H. D.; Wang, J. Y.; Zhang, H. J.; Hu, X. B.; Burns, P.; Piper, J. A. *Chem. Phys. Lett.* **2002**, *361*, 499−503. (c) Krebs, J. K.; Happek, U. *J. Lumin.* **2001**, *94*, 65−68. (d) Jiang, H. D.; Li, J.; Wang, J. Y.; Hu, X.-B.; Liu, H.; Teng, B.; Zhang, C.-Q.; Dekker, P.; Wang, P. *J. Cryst. Growth* **2001**, *233*, 248−252. (e) Lebedev, V. A.; Voroshilov, I. V.; Ignatiev, B. V.; Gavrilenko, A. N.; Isaev, V. A.; Shestakov, A. V. *J. Lumin.* **2000**, *92*, 139−144. (f) Dominiak-Dzik, G.; Ryba-Romanowski, W.; Gołąb, S.; Macalik, L.; Hanuza, J.; Pajączkowska, A. *J. Mol. Struct.* **2000**, *555*, 213−225. (g) Zhang, H. J.; Meng, X. L.; Zhu, L.; Wang, P.; Liu, X. S.; Yang, Z. H.; Dawes, J.; Dekker, P. *Phys. Status Solidi A* **1999**, *175*, 705−710. (h) Montoya, E.; Lorenzo, A.; Bausá, L. E. *J. Phys.: Condens. Matter* **1999**, *11*, 311−320. (i) Montoya, E.; Sanz-Garciá, J. A.; Bausá, L. E. *Spectrochim. Acta, Part A* **1998**, *54*, 2081−2085.

indicate that the ligand-field splitting of the f orbitals is not sensitive to the electronic differences between the neutral phen and bpy ligands. The fact that the positions and intensities of the shorter wavelength absorptions centered at 17300 $cm^{-1}$ ($\epsilon$ 130) and 24750 $cm^{-1}$ ($\epsilon$ 2400) are also insensitive to the identity of the diimine ligand suggests that neither transition is attributable to a metal (f)-to-diimine ($\pi^*$) charge transfer. These bands could be attributable to charge-transfer transitions localized on the ytterbocene portion of the $[(C_5Me_5)_2Yb(diimine)]^+$ adducts and/or metal-centered 4f $\rightarrow$ 5d transitions. It should be noted that the electronic absorption spectra of the related complexes $(C_5Me_5)_3Yb$ and $(C_5Me_5)_3Yb(L)$ [L = THF, THT, $PEt_3$, and pyrrolidine] each exhibit a $\pi(C_5Me_5)$-to-metal (f) charge-transfer band that is comparable in energy and intensity to the 17300 $cm^{-1}$ band of the $[(C_5Me_5)_2Yb(diimine)]^+$ adducts.[15] We are currently investigating the optical properties of other ytterbocene adducts to definitively assign the bands in this region.

Under the $C_{2v}$-symmetry ligand fields of the $[(C_5Me_5)_2Yb(diimine)]^+$ complexes, the orbital degeneracies of both the $^2F_{7/2}$ ground-state term and the $^2F_{5/2}$ excited-state term are completely lifted, yielding two manifolds of crystal-field states: the $^2F_{7/2}$ term is split into four levels with spin degeneracy (i.e., Kramers' doublets) and the $^2F_{5/2}$ term into three.[16] In the simplest case, the energetic splitting between the crystal-field levels of the $^2F_{7/2}$ term is sufficiently large that thermal population of the higher lying levels within the $^2F_{7/2}$ manifold can be neglected (i.e., $\Delta E \gg kT$), and the absorption spectrum is expected to exhibit three bands corresponding to transitions from the lowest energy $^2F_{7/2}$-derived level to the orbitally split components of the $^2F_{5/2}$ term. Thus, the absorption spectrum provides a direct measure of the splitting between the crystal-field levels of the $^2F_{5/2}$ term. At smaller crystal-field splittings within the $^2F_{7/2}$ ground-state manifold (i.e., $\Delta E \approx kT$), thermal population of the higher lying levels of the $^2F_{7/2}$ term increases, and concomitantly, bands corresponding to transitions from higher lying thermally populated $^2F_{7/2}$-derived levels to the $^2F_{5/2}$ manifold of states will occur at lower energy.

The electronic absorption spectra of the $[(C_5Me_5)_2Yb(bpy)]^+$ and $[(C_5Me_5)_2Yb(phen)]^+$ cations between 9000 and 12500 $cm^{-1}$ (Figure 2) exhibit several features, with the bands at ca. 9950, 10225, and 10470 $cm^{-1}$ having considerably more intensity ($\epsilon$ 50−200) than the others ($\epsilon \leq 10$). The bands within this triad, labeled 1−3 in Figure 2, are assigned to transitions from the lowest lying level of the $^2F_{7/2}$ ground-state term to the three crystal-field levels of the $^2F_{5/2}$ excited-state term. From the spacings between adjacent bands in this triad it is inferred that the separation between adjacent levels of the $^2F_{5/2}$ term is ca. 235 $cm^{-1}$. The lack of additional bands with appreciable intensity to lower energy of this triad suggests that the separation between the lowest energy $^2F_{7/2}$ levels is sufficiently large that only the lowest level is populated to any appreciable extent (i.e., $\Delta E > kT$).[17] In the absence of low-temperature emission data, which provide a direct probe of the $^2F_{7/2}$ ground-state term, it is difficult to unequivocally quantify the separations between the $^2F_{7/2}$-derived crystal-field levels. The weaker features observed in this region are presumably vibronic contributions built on bands 2 and 3. In particular, the blue edges of bands 2 and 3 clearly exhibit progressions of ca. 60 $cm^{-1}$; the low frequency of this progression suggests that it corresponds to a skeletal deformation of the coordination environment about the Yb center. In addition, there are two features at ca. 10830 and 11090 $cm^{-1}$ in the spectra of both cations. The fact that the spacing between these features (ca. 260 $cm^{-1}$) is similar to that between bands 2 and 3 (ca. 245 $cm^{-1}$) suggests that they correspond to separate vibronic origins of a 600 $cm^{-1}$ vibration built on bands 2 and 3. These features cannot be assigned to any specific mode(s) solely on the basis of the existing data.

The spectral pattern (number of bands and relative intensities of the bands) observed for the f $\rightarrow$ f transitions in these ytterbocene adducts is very similar to that seen in other $Yb^{3+}$ complexes. For example, the high-resolution absorption spectrum recently reported for the tris(2,6-pyridinedicarboxylate) complex[18] in the f $\rightarrow$ f region ($\sim$10250 $cm^{-1}$) is dominated by three bands corresponding to the transitions from the lowest lying level in the $^2F_{7/2}$ ground-state manifold to the three levels in the $^2F_{5/2}$ excited-state manifold. Notably, the comparatively low intensity and broadness of bands 2 and 3 observed for the tris(2,6-pyridinedicarboxylate) and $[(C_5Me_5)_2Yb(diimine)]^+$ complexes appear to be features common to the $^2F_{7/2} \rightarrow {}^2F_{5/2}$ triads of other $Yb^{3+}$ compounds.[14] It should also be noted that in many cases the spacing between the levels in the $^2F_{7/2}$ manifold is sufficiently small that transitions originating from the higher lying levels of the $^2F_{7/2}$ manifold are readily observed in room-temperature absorption spectra, as is the case for the tris(2,6-pyridinedicarboxylate) complex ($\Delta E \approx$ 100 $cm^{-1}$). The fact that no such bands are observed in the spectra of the $[(C_5Me_5)_2Yb(diimine)]^+$ complexes suggests that the crystal field generated by this coordination environment is significantly stronger than that in, for example, the tris(2,6-pyridinedicarboxylate) complex, leading to larger splittings between the levels in the $^2F_{7/2}$ manifold. Emission spectral studies of these $[(C_5Me_5)_2Yb(diimine)]^+$ complexes are under way to characterize the energetics of the $^2F_{7/2}$ manifold.

The electronic absorption spectra of the neutral diimine−ytterbocene complexes $(C_5Me_5)_2Yb(bpy)$ and $(C_5Me_5)_2Yb(phen)$ (Figure 3) are considerably more complicated than their cationic counterparts principally because of the presence of additional electronic states derived from the unpaired electron localized on their respective diimine ligands. Consequently, the spectra of $(C_5Me_5)_2Yb(bpy)$ and $(C_5Me_5)_2$-

(15) Schlesener, C. J.; Ellis, A. B. *Organometallics* **1983**, *2*, 529−534.
(16) Gerloch, M.; Constable, E. C. *Transition Metal Chemistry*; VCH: Weinheim, Germany, 1995.
(17) The intensities of the extremely weak features to the red of band 1 (at 9700 and 9790 $cm^{-1}$) are inconsistent with assignment to f $\rightarrow$ f transitions originating from thermally populated levels of the $^2F_{7/2}$ ground-state term. This conclusion is based on the fact that thermal population of higher energy $^2F_{7/2}$-derived levels is expected to be significant ($n_2/n_1 \approx 0.3$ at 300 K) for cases in which the separation between the lowest energy $^2F_{7/2}$ levels is <250 $cm^{-1}$.
(18) Reinhard, C.; Güdel, H. U. *Inorg. Chem.* **2002**, *41*, 1048−1055.

Yb(phen) are dominated by intense absorption bands arising from diimine-localized $\pi \rightarrow \pi^*$ and $\pi^* \rightarrow \pi^*$ transitions. The bands attributable to these transitions are similar in energy and intensity to those reported for their respective free diimine radical anions: the bands centered at 11235, 19840, and 25975 $cm^{-1}$ in the spectrum of $(C_5Me_5)_2Yb(bpy)$ correspond to bands observed in the spectrum of Na(bpy),[1,19] whereas the bands located between 12500 and 28500 $cm^{-1}$ in the spectrum of $(C_5Me_5)_2Yb(phen)$ correspond to those reported for Li(phen).[20] In both cases, these diimine-localized bands exhibit weakly resolved vibronic progressions of ca. 1200 $cm^{-1}$ that correspond to distortions localized on the diimine ligands.

The electronic absorption spectra of $(C_5Me_5)_2Yb(bpy)$ and $(C_5Me_5)_2Yb(phen)$ also exhibit moderately intense bands ($\epsilon \approx 1000$) centered near 5000 $cm^{-1}$ that are assigned as $\pi^*$-(diimine) $\rightarrow$ f ligand-to-metal charge-transfer transitions (LMCTs). These electronic excited states are the converse of the spontaneous ground-state charge-transfer process. The absorption bands exhibit weakly resolved vibronic progressions of ca. 1500−1600 $cm^{-1}$ that presumably correspond to a convolution of several vibrations localized on the diimine ligands. The fact that the progressions observed in these bands are of higher frequency than those observed in the $\pi \rightarrow$ p* and $\pi^* \rightarrow$ p* bands (ca. 1200 $cm^{-1}$) is consistent with the orbital nature of the $[(\pi^*)^1(f)^{13}] \rightarrow [(\pi^*)^0(f)^{14}]$ LMCT excited state, in which the bonding of the diimine ligand is expected to be stronger due to a depopulation of the $\pi^*$ orbital. The charge-transfer assignment for these bands is also consistent with the electrochemical data (Table 1 and eq 1) that show the corresponding separation between the ligand $\pi^*$ oxidation wave and the metal f orbital reduction wave is 0.79 V or ∼6400 $cm^{-1}$.

In addition to the $\pi \rightarrow \pi^*/\pi^* \rightarrow \pi^*$ and LMCT bands, the electronic absorption spectra of the neutral $(C_5Me_5)_2Yb$-(diimine) complexes are expected to exhibit f $\rightarrow$ f transitions since the metal centers retain the $f^{13}$ electronic configurations found in the cationic adducts. Given the structural similarities between the neutral and cationic congeners, it is anticipated that the energies of their f $\rightarrow$ f transitions should be comparable to those of their respective cations. In the case of $(C_5Me_5)_2Yb(bpy)$, the intense $\pi^* \rightarrow \pi^*$ band centered at 11235 $cm^{-1}$ obscures the 9000−12500 $cm^{-1}$ region in which the f $\rightarrow$ f bands are expected to lie (vide supra). In the case of the $(C_5Me_5)_2Yb(phen)$ complex, the phen-localized bands are sufficiently removed from this region (Figure 3), revealing two sharp, relatively intense f $\rightarrow$ f bands at 9940 nm ($\epsilon$ 650) and 11225 nm ($\epsilon$ 1600) and a weaker f $\rightarrow$ f band at 10720 nm ($\epsilon$ 97). The energetic proximity of these f $\rightarrow$ f bands in the phenanthroline adduct and the lowest energy $\pi^* \rightarrow \pi^*$ band of $(C_5Me_5)_2Yb(bpy)$ suggests that the $\pi^* \rightarrow \pi^*$ band profile in the bipyridine adduct may in fact contain underlying contributions from f $\rightarrow$ f bands similar in energy and intensity to those in the phenanthroline adduct.

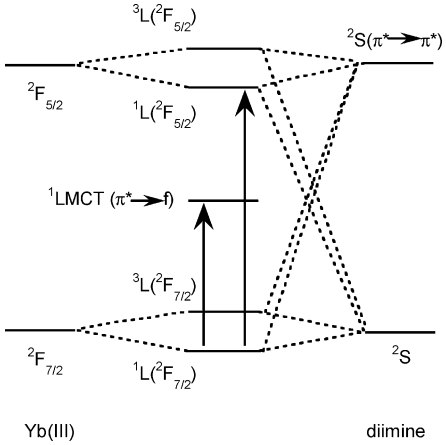


**Figure 4.** Proposed energy level diagram for the electronic states derived from mixing between metal- and diimine-localized spin states in the neutral $(C_5Me_5)_2Yb$(diimine) adducts.

There are two noteworthy aspects of the f $\rightarrow$ f bands in the neutral $(C_5Me_5)_2Yb(phen)$ complex. First, the energies of the spectral bands (centered at ca. 11000 $cm^{-1}$) and the separations between adjacent f $\rightarrow$ f bands (ca. 510 and 780 $cm^{-1}$) are significantly perturbed relative to the values found for $[(C_5Me_5)_2Yb(phen)]^+$ (ca. 10250 and 235 $cm^{-1}$, respectively). This could simply reflect the difference in charge between $(C_5Me_5)_2Yb(phen)$ and $[(C_5Me_5)_2Yb(phen)]^+$ or, more likely, the difference in the ligand-field strength of phen versus the phen radical anion. Second, the intensities in these bands for the neutral complex are 5−10 times greater than observed in the corresponding bands for the cationic complex.

The unusually large oscillator strengths of the f $\rightarrow$ f transitions of $(C_5Me_5)_2Yb(phen)$ can qualitatively be rationalized on the basis of an exchange model that accounts for the effect of spin−spin correlation on the intensities of absorption bands. A similar model has been used to explain the anomalous intensity of the spin-forbidden $^4A_{2g} \rightarrow {}^2E_g$ ligand-field bands of certain chromium(III) chromophores that possess radical anion ligands.[21] In the absence of exchange coupling between the metal $^2F$ spin states and the diimine-localized $^2S$ spin states, transitions between the $^2F_{7/2}$ and $^2F_{5/2}$ manifolds are rigorously spin-allowed (i.e., doublet−doublet) but are expected to carry little intensity due to the intrinsic parity-forbidden character of f $\rightarrow$ f transitions. Under an antiferromagnetic exchange-coupling mechanism, the ground- and excited-state $^2F$ spin states mix with the diimine-localized $^2S$ spin states (Figure 4) to yield the singlet and triplet spin states $^1L(^2F_{7/2})$,$^3L(^2F_{7/2})$,$^1L(^2F_{5/2})$, and $^3L(^2F_{5/2})$. (We have adopted the $^{(2S+1)}L(^2F_J)$ labeling scheme to emphasize the spin multiplicities and $^2F_J$ parentages of these states, which are derived from linear combinations of the $^2F$ and $^2S$ spin states.) Importantly, the spin correlation allows the $^1$LMCT and $^1L(^2F)$ states to mix, and transitions between the crystal-field levels of $^1L(^2F_{7/2})$ and $^1L(^2F_{5/2})$ can steal

(19) König, E.; Kremer, S. *Chem. Phys. Lett.* **1970**, *5*, 87−90.
(20) Turró, C.; Chung, Y. C.; Leventis, N.; Kuchenmeister, M. E.; Wagner, P. J.; Leroi, G. E. *Inorg. Chem.* **1996**, *35*, 5104−5106.
(21) (a) Tsukahara, Y.; Iino, A.; Yoshida, T.; Suzuki, T.; Kaizaki, S. *J. Chem. Soc., Dalton Trans.* **2002**, 181−187. (b) Tsukahara, Y.; Kamatani, T.; Iino, A.; Suzuki, T.; Kaizaki, S. *Inorg. Chem.* **2002**, *41*, 4363−4370. (c) Benelli, C.; Dei, A.; Gatteschi, D.; Güdel, H. U.; Pardi, L. *Inorg. Chem.* **1989**, *28*, 3089−3091.

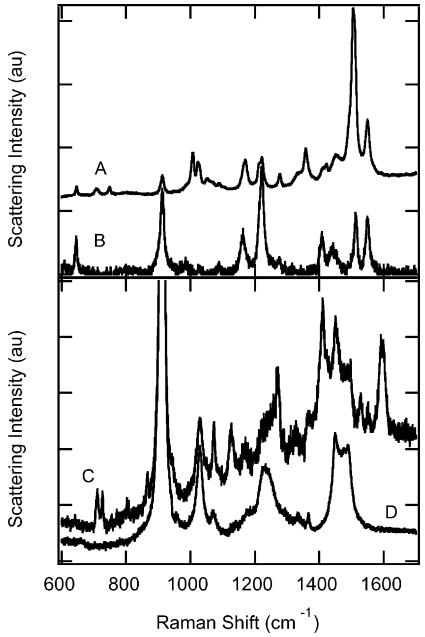


**Figure 5.** Raman spectra for the neutral diimine adducts of ytterbocene: (A) ~0.1 M $(C_5Me_5)_2Yb(bpy)$ in THF obtained with 514 nm $Ar^+$ laser excitation; (B) ~0.1 M $(C_5Me_5)_2Yb(bpy)$ in THF obtained with 753 nm Ti:sapphire laser excitation; (C) microcrystalline $(C_5Me_5)_2Yb(phen)$ immersed in THF obtained with 514 nm $Ar^+$ laser excitation; (D) neat THF obtained with 514 nm $Ar^+$ laser excitation.

intensity from the $[(\pi^*)^1(f)^{13}] \rightarrow [(\pi^*)^0(f)^{14}]$ transition, denoted in Figure 4 as $^1L(^2F_{7/2}) \rightarrow {}^1$LMCT. Since the intensity enhancement of the f → f bands is proposed to derive from the exchange coupling between spins localized on the Yb center and the diimine ligand, it is anticipated that the extent of intensity enhancement will track with the magnitude of the antiferromagnetic coupling constant *J*. We are currently working to exploit this relationship to quantify *J* for the $(C_5Me_5)_2Yb(diimine)$ complexes.

**Resonance Raman Spectroscopy.** In molecular systems that have intense electronic absorption bands associated with ligand-localized $\pi$ (or $\pi^*$) → $\pi^*$ transitions and/or metal−ligand charge-transfer transitions (i.e., electronic transitions between states having substantially different potential energy distributions), it is frequently possible to utilize resonance Raman spectroscopy as a probe of the vibrational potential energy distribution in the ground state and the nature and structure of the excited electronic states from which the resonance effect is derived. Raman vibrational spectra have been acquired for the bpy and phen adducts of ytterbocene. The bpy adduct is quite soluble in THF, and spectra were obtained from concentrated (~0.1 M) solutions. The phen adduct is only sparingly soluble in all common solvents, so the Raman data for this adduct were obtained on a finely divided powder settled in the bottom of a capillary containing THF. Representative spectral data are shown in Figure 5. Raman data were also collected for a concentrated THF solution (~0.1 M) of the THF adduct $(C_5Me_5)_2Yb(THF)_n$. The THF adduct has no intense electronic absorption features in the visible region of the spectrum. Thus, even though the solution sample was concentrated, no vibrational modes associated with the complex were observed under visible wavelength laser excitation. The observed spectrum is identical to that obtained for neat THF.

The spectrum of the neutral bipyridine adduct obtained with 514 nm excitation (Figure 5A) exhibits a wealth of vibrational bands. This excitation wavelength is in resonance with one of the $\pi^* \rightarrow \pi^*$ transitions discussed above, and the Raman spectrum clearly demonstrates a strong enhancement effect from this resonant electronic transition. Note that the band intensities from the complex modes (~0.1 M) are comparable to that for the most intense solvent band at 914 $cm^{-1}$, demonstrating the presence of resonance enhancement. A resonance-enhanced spectrum is also obtained for the bpy adduct using 753 nm excitation (Figure 5B). Further discussion of the differences between these bpy adduct spectra is provided below. The observed Raman scattering for the phen adduct using 514 nm excitation (Figure 5C) is significantly weaker than that seen in the bpy adduct. Nonetheless, there are still many vibrational modes attributable to the phen complex with intensities comparable to those for the modes of the solvent in which the solid complex is immersed, thereby also suggesting some degree of resonance enhancement in the spectrum of the phen adduct.

The importance of these diimine ligands in transition-metal coordination chemistry, photochemistry, and photophysics[22−28] has led to extensive steady-state and time-resolved Raman and resonance Raman studies on both metal−diimine complexes and the free ligands. Thus, there is a wealth of information upon which to draw to assist in the interpretation of these resonance Raman data for the ytterbocene adducts. Previous bulk magnetic susceptibility data and electronic absorption spectroscopic data presented here and previously[1,3] suggest that the diimine ligands in these neutral ytterbocene adducts are best formulated as metal-complexed radical anions. The Raman vibrational data presented here provide an ideal test of this assignment since the spectra should strongly resemble those of the alkali-metal-reduced bpy and phen species. The mode energies and qualitative intensity patterns from the Raman spectra of the bpy− and phen− ytterbocene adducts are summarized and compared to literature data[20,29,30] for the $Li^+(diimine^{\bullet-})$ species in Table 2.

The Raman spectral data for $(C_5Me_5)_2Yb(bpy)$ are clearly consistent with the assignment of the bpy ligand as a reduced radical anion. There is a high correlation between the modes observed for this ytterbocene adduct and those for the bpy radical anion prepared by lithium metal reduction, and the energy match is also quite good for the correlated modes

(22) Forster, L. S. *Coord. Chem. Rev.* **2002**, *227*, 59−92.
(23) Balzani, V.; Juris, A. *Coord. Chem. Rev.* **2001**, *211*, 97−115.
(24) Kaes, C.; Katz, A.; Hosseini, M. W. *Chem. Rev.* **2000**, *100*, 3553−3590.
(25) Sammes, P. G.; Yahioglu, G. *Chem. Soc. Rev.* **1994**, *23*, 327−334.
(26) Sun, H.; Hoffman, M. Z.; Mulazzani, Q. G. *Res. Chem. Intermed.* **1994**, *20*, 735−754.
(27) Constable, E. C. *Adv. Inorg. Chem.* **1989**, *34*, 1−63.
(28) Sliwa, W. *Heterocycles* **1979**, *12*, 1207−1237.
(29) Danzer, G. D.; Golus, J. A.; Strommen, D. P.; Kincaid, J. R. *J. Raman Spectrosc.* **1990**, *21*, 3−8.
(30) Schoonover, J. R.; Omberg, K. M.; Moss, J. A.; Bernhard, S.; Malueg, V. J.; Woodruff, W. H.; Meyer, T. J. *Inorg. Chem.* **1998**, *37*, 2585−2587.

**Table 2.** Comparison of the Raman Shifts and Scattering Intensities for Diimine Ligand Modes from Resonance-Enhanced Spectra for $(C_5Me_5)_2Yb$ Adducts versus Ligand Radical Anions from Lithium Metal Reductions at Various Excitation Wavelengths[a]

| $(C_5Me_5)_2Yb(bpy)$ | | | | $Li^+bpy^{\bullet-}$ (ref 29) | | $(C_5Me_5)_2Yb(phen)$ | | $Li^+phen^{\bullet-}$ (ref 20) | | | | $Li^+ phen^{\bullet-}$ (ref 30) | |
|---|---|---|---|---|---|---|---|---|---|---|---|---|---|
| 514 nm | | 753 nm | | 407 nm | | 514 nm | | 407 nm | | 351 nm | | 407 nm | |
| 646 | w | 645 | m | nr | | | | | | | | | |
| 709 | w | | | nr | | | | | | | | | |
| 749 | w | | | 745 | s | 711 | m | nr | | nr | | nr | |
| 989 | w, sh | 983 | w | 991 | s | 727 | m | nr | | nr | | nr | |
| 1007 | m | | | 1018 | m | 803 | w | nr | | nr | | nr | |
| 1024 | m | 1028 | w | 1030 | m | 866 | w | nr | | nr | | nr | |
| 1052 | w | | | 1050 | | | | 1043 | vs | 1044 | m | nr | |
| 1089 | w | 1088 | w | 1081 | w | | | 1061 | m | | | nr | |
| 1164 | m, sh | 1162 | m | 1162 | w | 1073 | m | | | | | nr | |
| 1170 | m | | | | | 1125 | m, br | 1122 | w | 1128 | vw | 1119 | m |
| 1214 | m, sh | | | 1205 | s | 1170 | w | 1174 | w | 1178 | w | | |
| 1221 | m | 1221 | s | | | | | 1221 | mw | 1217 | w | 1212 | m |
| 1277 | w | 1275 | w | 1275 | s | | | | | | | | |
| | | | | 1292 | w | 1270 | m | 1272 | s | 1273 | s | 1281 | m |
| 1338 | w, sh | | | 1350 | m | 1330 | w, br | 1343 | w | 1344 | w | 1335 | m |
| 1358 | m | | | 1363 | w, sh | 1370 | w, br | 1390 | m | | | | |
| 1412 | w, sh | 1408 | m | 1412 | m | 1411 | s | 1414 | w | | | 1421 | m |
| 1421 | w | | | | | 1450 | m | 1449 | vs | 1442 | m | 1453 | m |
| 1453 | w, br | 1440 | w,b | 1438 | w | | | 1506 | w | 1499 | m | 1515 | m |
| 1496 | m,sh | | | 1485 | s | 1530 | w | 1539 | w | 1539 | vw | 1543 | m |
| 1506 | s | 1513 | m | 1502 | m | 1550 | w | | | | | | |
| | | | | 1511 | w, sh | | | 1575 | vw | 1576 | s | | |
| 1549 | m | 1550 | m | 1554 | s | 1591 | s, br | | | 1606 | s | 1587 | w |

[a] Mode energies are in $cm^{-1}$. Intensity legend: w = weak, m = moderate, s = strong, vs = very strong, br = broad, sh = shoulder, nr = not within spectral range of reported data.

(Table 2). The selective resonance enhancement in only these bpy-related modes is also an indication that the excited states in which the exciting laser lines are in resonance are ones that are highly localized on the bpy ligand (i.e., $\pi^* \rightarrow \pi^*$ transitions as discussed above). Only three bands in the ytterbocene adduct spectrum (1170, 1221, and 1421 $cm^{-1}$) have no clearly analogous modes in the $Li^+(bpy^{\bullet-})$ spectrum. It is unlikely that these modes are associated with the $C_5Me_5$ ligands as these would not be expected to be enhanced in resonance with the bpy-localized excited states, and further, no such modes are observed in the Raman spectra of the $(C_5Me_5)_2Yb(THF)_n$ complex. Furthermore, while previous vibrational spectroscopic studies of alkali- and transition-metal complexes containing $C_5Me_5$ ligands[31,32] do report a strong polarized Raman mode associated with this ligand at ~1430 $cm^{-1}$, there are no other $C_5Me_5$-localized modes in the range that encompasses 1170 and 1221 $cm^{-1}$.

The change in the relative intensities in the bipyridine radical anion modes in the ytterbocene adduct is quite pronounced on going from a 514 to a 753 nm excitation wavelength (Figure 5 and Table 2). Note, however, that these two wavelengths are in resonance with two different electronic absorption bands (Figure 3). Although both absorption bands have been assigned to $\pi^* \rightarrow \pi^*$ states originating from the LUMO on bpy, the states involve different terminal $\pi^*$ orbitals; the 753 nm spectrum is in resonance with the lowest lying state, whereas the 514 nm spectrum is in resonance with the next higher lying state. In a simple one-electron description these terminal $\pi^*$ orbitals are the LUMO + 1 and LUMO + 2 derived from the neutral bipyridine molecule. Ab initio molecular orbital calculations for the neutral bipyridine ligand clearly demonstrate that the nodal patterns in these two orbitals are quite different.[33] Therefore, one would expect the Franck−Condon factors that govern the resonance Raman intensities to be quite different between these two electronic states. The most intense mode in the 514 nm spectrum occurs at 1506 $cm^{-1}$. In the description adopted by Kincaid et al.[29] for the bipyridine radical anion and the MLCT excited state of $[Ru(bpy)_3]^{2+}$, this mode is $\nu_6$ and involves a substantial contribution from a stretching motion of the bridging ($C_2$–$C_{2'}$) ring bond. The resonant electronic transition from the LUMO to the LUMO + 2 involves a change from a bonding interaction between these two carbon atoms in the LUMO to an antibonding interaction in LUMO + 2. In the 753 nm Raman spectrum, the 1506 $cm^{-1}$ mode is relatively weak and the most intense mode occurs at 1221 $cm^{-1}$ ($\nu_{11}$ in Kincaid's scheme). This mode entails substantial distortions orthogonal to the vector defined by $C_5-C_2-C_{2'}-C_{5'}$. The resonant electronic transition in this case (LUMO to LUMO + 1) involves a change from orbitals in-phase to orbitals out-of-phase along this molecular axis. Thus, in both spectra, the most intense modes reflect the nature of the terminal orbital in the resonant electronic transition. Further exploration of the details of mode assignments and resonance enhancement patterns is ongoing and will be presented in subsequent publications.

The Raman vibrational data for metal complexes of the phenanthroline ligand, including those of the ligand radical anion prepared by alkali-metal reduction, have been a topic of considerable controversy for a number of years.[20,30] The controversy stems from the surprising overall weakness of

(31) Bencze, É.; Mink, J.; Németh, C.; Herrmann, W. A.; Lokshin, B. V.; Kühn, F. E. *J. Organomet. Chem.* **2002**, *642*, 246−258.
(32) Bencze, É.; Lokshin, B. V.; Mink, J.; Herrmann, W. A.; Kühn, F. E. *J. Organomet. Chem.* **2001**, *627*, 55−66.
(33) Endicott, J. F.; Schlegel, H. B.; Uddin, M. J.; Seniveratne, D. S. *Coord. Chem. Rev.* **2002**, *229*, 95−106.

the resonance Raman effect for phenanthroline ligand modes in MLCT excited states of complexes such as $[Ru(phen)_3]^{2+}$ and from an apparent difficulty in distinguishing ground-state ligand modes from those of the charge-transfer excited state that should take on the same general properties as the chemically prepared radical anion. Additionally, recent theoretical and spectroscopic studies have confirmed that there are two nearly degenerate low-lying $\pi^*$ orbitals for the phenanthroline ligand having differing orbital symmetries ($a_2$ and $b_1$) and thus different nodal patterns.[34−36] Interference effects arising from nearly degenerate states derived from these orbitals could lead to de-enhancement phenomena that could both weaken and complicate phenanthroline resonance Raman responses.[37]

The relatively weak resonance Raman effect reported for other transition-metal−phenanthroline complexes appears to persist in the ytterbocene adduct of phenanthroline as evidenced by the spectrum shown in Figure 5C. Nonetheless, the basic interpretation of these data in comparison to those reported for $Li^+(phen^{\bullet-})$ (Table 2) is that the diimine ligand in the ytterbocene−phen adduct is best regarded as a reduced radical anion consistent with the other magnetic, spectroscopic, and electrochemical data. As in the comparison of the vibrational data for $bpy^{\bullet-}$ vs $(C_5Me_5)_2Yb(bpy)$, for the phenanthroline analogues there is an excellent correlation between the phenanthroline modes in the adduct spectrum and those in the spectrum of the radical anion. Note that there is also a strong excitation wavelength dependence on the intensities in the literature spectra for the radical anion, suggesting that these excitations probe different $\pi^* \rightarrow \pi^*$ excited states as was the case for $(C_5Me_5)_2Yb(bpy)$. In fact, the data collected for $(C_5Me_5)_2Yb(phen)$ utilizing 514 nm excitation are likely derived from resonance with still another, lower lying $\pi^* \rightarrow \pi^*$ state having a different nodal pattern. Detailed potential energy distributions and vibrational assignments are not readily available for the phenanthroline ligand and its radical anion. Thus, even qualitative conclusions regarding these differing resonance Raman intensity patterns versus excitation wavelength are not possible. It is, however, noteworthy that the spin population differs substantially in the $a_2$ versus $b_1$ LUMOs on phenanthroline, with the former having significanly less electron density on the coordinating nitrogens than the latter.[34] While it is not known which of these orbitals lies lowest in the ytterbocene adduct or to what extent, if the electron resident on the phenanthroline ligand is predominantly in the $a_2$ LUMO, this might be a cause for the apparent lesser spin coupling between the ligand $^2S$ and metal $^2F$ states found in the magnetic data for this complex relative to the bipyridine adduct.

## Summary

The cyclic voltammetric data for $(C_5Me_5)_2Yb(bpy)$ and $(C_5Me_5)_2Yb(phen)$ clearly demonstrate a remarkable stabilization of their respective diimine LUMOs and concomitant destablization of f orbitals on the metal that make the spontaneous ground-state charge-transfer process energetically favorable. The data from the f → f spectral region for the cationic adducts indicate that the f orbital splitting in these species is not sensitive to the differences in the electronic structures of bipyridine versus phenanthroline ligands. The unexpectedly strong intensities of the f → f bands for the neutral complexes can be explained using a simple intensity-borrowing model that is based on the antiferromagnetic coupling model used to explain the magnetic behavior of these complexes. Despite the strong spin−spin correlation inferred from the intensities of the f → f bands, the coupling is still weak enough to distinguish bands attributable to f → f transitions (in cases where the overlap of bands does not preclude this), ligand-localized transitions, and the LMCT. The Raman data provide an unequivocal confirmation of the radical anion nature of the diimine ligand in these ytterbocene adducts, and the sensitivity of the intensity patterns to changes in the resonant electronic transition reflects the differences in the electron-density distribution in the higher lying ligand-localized $\pi^*$ orbitals. However, none of the data reported here (electrochemical, electronic absorption, or resonance Raman) provide a clear differentiation between the electronic structure in the bipyridine versus phenanthroline ligand adducts that would readily explain the apparent difference in the extent of coupling of the spin states on the ligand radical anion and the f orbital manifold on the metal. Additional investigations are currently under way using other imine-type ligands to vary the symmetry and crystal-field strength of the ytterbocene adducts to further explore this interesting electronic-structure problem.

**Acknowledgment.** Funding for this work was provided by the Los Alamos National Laboratory's Laboratory Directed Research and Development program. All work was performed at Los Alamos National Laboratory under contract with the University of California (Contract No. W-7405-ENG-36). We gratefully acknowledge Dr. Jaqueline L. Kiplinger for providing the $[(n\text{-}C_4H_9)_4N][B(C_6F_5)_4]$ salt for the electrochemical investigations and Prof. Richard A. Andersen of the Chemistry Department at the University of California, Berkeley, for providing samples of $(C_5Me_5)_2Yb(bpy)$ and helpful preliminary discussions of research results.

IC030069I

(34) Ernst, S.; Vogler, C.; Klein, A.; Kaim, W.; Zališ, S. *Inorg. Chem.* **1996**, *35*, 1295−1300.
(35) Farrell, I. R.; Hartl, F.; Zališ, S.; Mahabiersing, T.; Vlček, A. *J. Chem. Soc., Dalton Trans.* **2000**, 4323−4331.
(36) Farrell, I. R.; van Slageren, J.; Zališ, S.; Vlček, A. *Inorg. Chim. Acta* **2001**, *315*, 44−52.
(37) Morris, D. E.; Woodruff, W. H. *J. Phys. Chem.* **1985**, *89*, 5795−5798.